

Green Chemistry

Accepted Manuscript



This article can be cited before page numbers have been issued, to do this please use: E. Peris, O. Okafor, E. Kulcinskaja, R. Goodridge, S. V. Luis, E. Garcia-Verdugo, E. O'Reilly and V. Sans, *Green Chem.*, 2017, DOI: 10.1039/C7GC02421E.



This is an Accepted Manuscript, which has been through the Royal Society of Chemistry peer review process and has been accepted for publication.

Accepted Manuscripts are published online shortly after acceptance, before technical editing, formatting and proof reading. Using this free service, authors can make their results available to the community, in citable form, before we publish the edited article. We will replace this Accepted Manuscript with the edited and formatted Advance Article as soon as it is available.

You can find more information about Accepted Manuscripts in the [author guidelines](#).

Please note that technical editing may introduce minor changes to the text and/or graphics, which may alter content. The journal's standard [Terms & Conditions](#) and the ethical guidelines, outlined in our [author and reviewer resource centre](#), still apply. In no event shall the Royal Society of Chemistry be held responsible for any errors or omissions in this Accepted Manuscript or any consequences arising from the use of any information it contains.



Journal Name

COMMUNICATION

Tuneable 3D printed bioreactors for transaminations under continuous-flow

Received 00th January 20xx,
Accepted 00th January 20xx

DOI: 10.1039/x0xx00000x

www.rsc.org/

Edgar Peris,^a Obinna Okafor,^{b,d} Evelina Kulcinskaja,^c Ruth Goodridge,^b Santiago V. Luis,^a Eduardo Garcia-Verdugo,^a Elaine O'Reilly,^c Victor Sans,^{b,d*}

A method to efficiently immobilize enzymes on 3D printed continuous-flow devices is presented. Application of these chemically modified devices enables rapid screening of immobilization mechanisms and reaction conditions, simple transfer of optimised conditions into tailored printed microfluidic reactors and development of continuous-flow biocatalytic processes. The bioreactors showed good activity (8-20.5 $\mu\text{mol h}^{-1} \text{mg}_{\text{enz}}^{-1}$) in the kinetic resolution of 1-methylbenzylamine, and very good stability (ca. 100 h under flow).

The development of biocatalytic processes is emerging as a new paradigm in the sustainable manufacturing of high value chemicals for the pharmaceutical industry.^{1, 2} The application of biocatalysts can provide alternative synthetic approaches to those relying on more traditional chemistry, reducing the need for toxic reagents, transition-metal catalysts and avoiding costly purification steps and protecting group manipulations.³ The immobilization of enzymes onto solid supports has facilitated the development of biocatalytic industrial processes, by simplifying the recovery and reuse of the enzymes and enabling their transition into continuous flow reactors.⁴⁻⁶ However, the number of commercially available systems is currently limited, mainly due to the absence robust immobilization strategies.

Additive manufacturing, commonly known as 3D printing, has the potential to enable the rapid assembly of complex reaction system geometries, which is often challenging using traditional manufacturing techniques.⁷ The development of 3D printed devices for chemical synthesis, coined "reactionware", has gained a great deal of attention in recent years,⁸ and continuous-flow reactors with varying degrees of sophistication have been described in the literature for a variety of applications.⁹⁻¹³ However, the chemical post-modification of printed devices has received much less

attention.¹⁴ The development of reliable methods for chemical modification has enormous potential to reduce cost and deliver functional devices for rapid screening of immobilized enzymes. Furthermore, the freedom of design inherent to 3D printing allows parallelized fast screening platforms to be combined with intensified continuous-flow reactors featuring advanced geometries and optimized mixing properties.

Here, we report the first example of modified 3D printed devices (Figure 1A) for the immobilization and application of ω -transaminase (ω -TA) enzymes in continuous-flow. The sequential chemical functionalization of the printed devices (Figure 1B) enables a fine control of the physico-chemical properties of the reactor surface, thus enabling diverse types of interaction with target enzymes and allowing rapid screening of experimental conditions. The strategy combines effective enzyme immobilization and reutilization with the efficiency of continuous-flow and represents a significantly more sustainable approach to the development of biocatalytic processes compared to those in traditional batch reactors.^{5b}

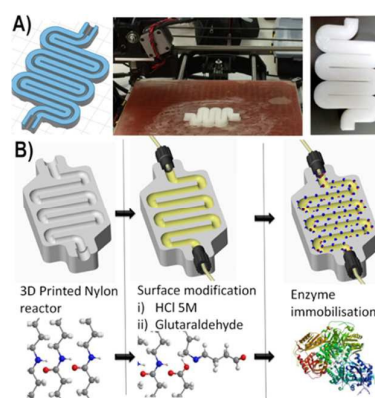


Figure 1. Schematic representation of the preparation of 3D printed bioreactors. A) Printing process of Nylon employing an FDM printer, including a CAD file of a simple fluidic device (left), the printing process (centre) and the device (right). B) Schematic representation of the post-functionalisation of the printed reactor.

^a Departamento de Química Inorgánica y Orgánica, Universitat Jaume I, 12071, Castellón de la Plana, Spain

^b Faculty of Engineering, University of Nottingham, NG7 2RD, Nottingham, UK.

^c School of Chemistry, University of Nottingham, NG7 2RD, Nottingham, UK.

^d GSK Carbon Neutral Laboratory, University of Nottingham, Nottingham, NG8 2GA, UK. E-mail: victor.sanssanggornin@nottingham.ac.uk

Electronic Supplementary Information (ESI) available: See DOI: 10.1039/x0xx00000x

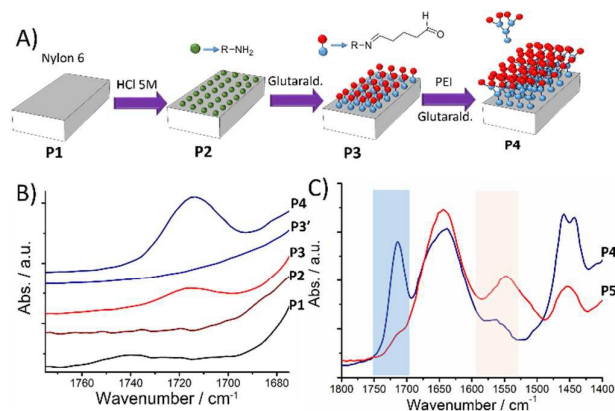


Figure 2. Chemical modification of 3D printed material for enzyme immobilization. A) A 3D printed nylon part (P1) was treated with HCl 5M (P2) and then the superficial amine groups were reacted with glutaraldehyde (P3) to generate covalent link points for the enzyme. The reaction with polyethyleneimine (PEI) (polymer P3') and glutaraldehyde led to a polymer with increased linkage points (P4). B) Detail of the aldehyde band in the ATR-IR spectra from polymers P1-P4. C) Disappearance of the aldehyde band (blue region) of polymer P4 in contact with a ω -TA enzyme and amide-II bands observed at 1550 cm^{-1} (brown region).

An extrusion based 3D printing platform, Lulzbot Taz 5, with commercially available nylon 6 filaments was employed to fabricate bespoke devices. The surface was sequentially modified to enable the adhesion of enzymes, allowing the design of biocatalytic systems for screening in multiple well-plate and continuous-flow biocatalytic reactors. Nylon is a particularly convenient immobilization matrix for enzymes.^{15, 16} It is inexpensive, chemically inert, non-toxic, has good mechanical properties and is commercially available in multiple formats. Indeed, several studies report the immobilization of various enzymes like proteases, glucosidases, endocellulases and laccases onto different nylon matrices.^{15, 17} Various types of nylon are widely employed for additive manufacturing. Powder based nylon 11/12 is commonly employed material of choice for selective laser sintering (SLS) methods.¹⁸ These platforms are capable of producing robust parts with highly intricate geometries and fine layer resolution of $100\text{ }\mu\text{m}$. Therefore, there is an untapped potential to develop 3D printed supported bioreactors fabricated in nylon.

The initial goal was to functionalise 3D printed nylon. To this end, small pieces of commercially available Nylon Taulman 645 ($1\times0.6\times0.2\text{ cm}$) were printed and chemically modified following the scheme shown in Figure 2A. After brief treatment with HCl (5M), a functional surface was generated with glutaraldehyde, as evidenced by the presence of a characteristic aldehyde C=O band at 1719 cm^{-1} in the ATR-IR spectra (Figure 2B, P3). This modification was accompanied with a change of colour from white to light orange. In order to increase the functionality of the surface, polymer P3 was treated with polyethylenimine (PEI, 60k Mn) to form the corresponding imine leading to multiple free amines at the nylon surface (Polymer P3'). The further reaction with glutaraldehyde led to a highly-functionalised polymer P4, characterized by the significant

increase in the intensity of the C=O band associated with this functionality (Figures 2B-C, spectra P4).

The application of transaminases for the synthesis of optically pure chiral amines from readily available ketones has received considerable attention from both the academic and industrial communities, due to the challenging nature of this transformation.¹⁹⁻²⁴ Additionally, there are only a handful of reports describing their successful application in continuous flow.²⁵⁻²⁸ We selected the commercially available (*R*)- ω -TA, ATA117, to demonstrate our flow methodology. The enzyme was supported following a literature procedure (see ESI) and the immobilization confirmed by ATR-FTIR (Figure 2, polymer P5). An assay was used to confirm that the enzyme had retained activity (see ESI).

A key advantage of the use of 3D printing is the ability to rapidly generate multiplexed reactors that can increase the experimental throughput, thus speeding up the discovery and optimization of new compounds or processes.²⁹ This can be invaluable for the rapid screening of immobilization conditions, which usually relies on trial and error approach, being time and resource intensive. Indeed, the use of microplate based immobilization techniques has been described to rapidly establish the best immobilization techniques for esterases.³⁰ Exploiting the same materials for enzyme immobilization and the development of 3D printed flow reactors has the potential to significantly speed up time and reduce labour intensive assays due to the rapid translation of immobilization conditions.

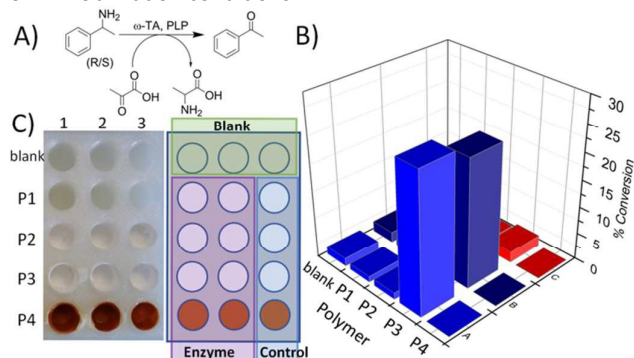


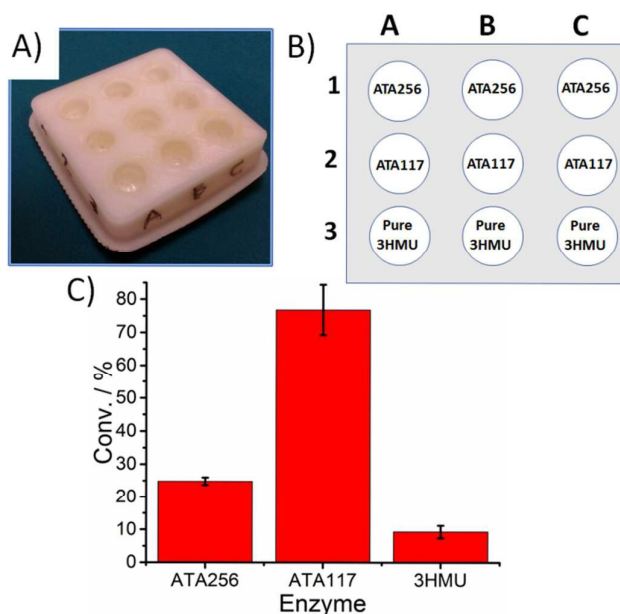
Figure 3. Evaluation of the effect of immobilisation on the enzymatic activity of an ω -TA ATA117. A) reaction scheme for the benchmark reaction. B) Experimental results obtained for the different immobilisation conditions. C) Image and scheme of the chemically modified 3D printed wells (left) and the experimental design (right), consisting of a combination of blank reactors without chemical modification nor enzyme (green box), control reactions in chemically modified wells without enzyme (blue box) and chemically modified wells containing enzyme (purple). Reaction conditions: Each well was filled with a $785\text{ }\mu\text{L}$ solution of methylbenzylamine (5mM) ((*R*)-MBA in wells 1 & 2 and (*Rac*)-MBA in well 3), pyruvate (5mM) and PLP (0.1mM) in potassium phosphate buffer, pH=8.0. Reactions run at $30\text{ }^{\circ}\text{C}$ for 17 hours.

A multi-well plate (dimensions: $1\text{ cm i.d.} \times 1\text{ cm height}$, Figure 3C) was manufactured in Nylon (Taulman 645). Four different immobilization strategies were simultaneously screened (see ESI, Figure S2 for the proposed immobilization mechanisms). The first row was left unmodified and without enzyme to function as a blank for the reaction. The wells of row 2 were maintained unmodified (i.e. with polymer P1) to study the

possible non-covalent immobilization directly on the surface by weak interactions (hydrogen bonds, hydrophobic effects, etc.). Polymer P2 (Figure 3C, row 3) provides a surface capable to immobilize the enzyme through ionic pairing and hydrogen bonds. Non-covalent immobilization is sometimes preferred to covalent immobilization as a minimal distortion of enzyme structures is expected. The covalent immobilization of the enzyme by polymer P3 in row 4 and multi-punctual covalent immobilization row 5. After the modifications, the wells of rows 2-5 and columns 1 and 2 were filled with a solution of a (*R*)- ω -TA (ATA117, 1 mg/ml solution of the enzyme in 0.1M K phosphate buffer pH=8.0, with 0.1 mM PLP). Column 3 was employed as a control, containing only buffer and PLP. The plate was left overnight at 4 °C. After this period, the wells were emptied and washed with buffer. Wells in rows 4 and 5 were then additionally washed with a solution of NaCl (0.5 M) for 2 hours to remove any non-covalently immobilized enzyme.

The conversion of (*R*)-methyl-benzylamine into acetophenone was selected as a model transamination reaction to evaluate the performance of the ω -TA immobilized in the nylon wells (Figure 3A). The wells were filled with 785 μ L of a solution containing the reagents required for the biotransformations (see figure 3 legend for details). After 17 hours, the solution was removed from the wells, extracted with ethyl acetate and analysed by GC/MS. The results obtained are summarized in the Figure 3B. The control experiments (row 1 and column 3) showed only residual activity (< 2%) indicating no catalytic activity from the different polymers without enzyme. Only polymer P4 (row 4, columns 1 and 2) showed some level of activity (ca. 25%). The ω -TA immobilized on the modified surface with higher number of superficial aldehydes, which can potentially bind to the enzyme in multiple points (row-5) did not exhibited any level of activity. This was rather surprising, and it might be due to the presence of multiple covalent bonds between the enzyme and the support inducing changes in the structure of the enzyme or due to the adsorption of the substrates. In light of these results, polymer P4 (glutaraldehyde functionalized nylon) appeared to be the more efficient way to immobilize the ω -TA tested. The diffusion of substrate outside the wells was visually observed, indicating an imperfect inter-bonding layer (see ESI TableS1).

A new type of Nylon 6 (Taulman 618), which showed better inter-layer adhesion, was employed to manufacture a new set of well plates with the same dimensions and to evaluate the effect on a small panel of ω -TAs. A plate containing 6 wells was printed and modified to generate the equivalent of polymer P4, called P4' for simplicity. Three different ω -TAs, two of them (*S*) selective (256 and 3HMU) and one (*R*) selective (ATA117) were immobilized in triplicate under same conditions previously employed. The benchmark reaction, the conversion of (*R*)- or (*S*)-methyl-benzylamine into acetophenone, was employed in order to compare the activity of the enzymes. The results demonstrated satisfactory reproducibility for the triplicate assays. The (*S*)-selective ω -TAs displayed a lower activity than the (*R*)-selective enzyme (ATA117 > 256 > 3HMU) (Figure 4). In summary, this simple screening highlighted



ATA117 as the most suitable ω -TA enzyme for immobilization by covalent attachment to 3D printing well-plate device (polymer P4').

Figure 4. A) 3D-printed Nylon wells used to perform the screening of the different enzymes. B) Representation of the enzyme distribution in the wells. C) Average conversion and standard deviation (error bars) observed for the three experiments of each of the enzymes tested. Conditions: 5mM (*R*)-MBA (in the case of ATA117) or *S*-MBA (in the case of ATA256 and 3HMU), 5mM pyruvic acid, 0.1mM PLP, r.t., 30 °C. 0.785 ml of a solution of the reagents in 0.1 M K phosphate buffer pH 8.0 was introduced in each well.

Crucially, the results of the screening can be readily transferred into continuous-flow micro-structured devices. The bioreactor devices were built in Nylon Taulman 618, Figure 4A, using the same platform described for the fabrication of the test wells. An iterative approach described in the ESI was employed to optimize the reactor manufacturing conditions. The nozzle temperature, build chamber temperature and model design were adjusted in order to produce robust leak-free devices. A 'track and hole' support structure (ESI, Table S1) was incorporated into the design of the reactor to break up the large surface area of the part printed per layer, aiming to minimize warping. This design also reduces temperature build up at the mid regions of the part as allows air flow through these areas. The reactor device was connected with PTFE tubing using rheodyne metal connectors.

The reactor modification was performed under stop-flow conditions for the HCl and glutaraldehyde solutions (see ESI for details). The immobilization of the enzyme was achieved via recirculation at 25 μ L·min⁻¹ a 15 mL of solution of ATA117 (5 mg/mL in 0.1 M of K phosphate buffer pH=8.0 and 0.1mM PLP) at r.t. for 24h. and washed with buffer solution afterwards. The analysis of the enzyme solution after the immobilization process indicated that 170 μ g of ω -TA were attached to the surface of the reactor channel.

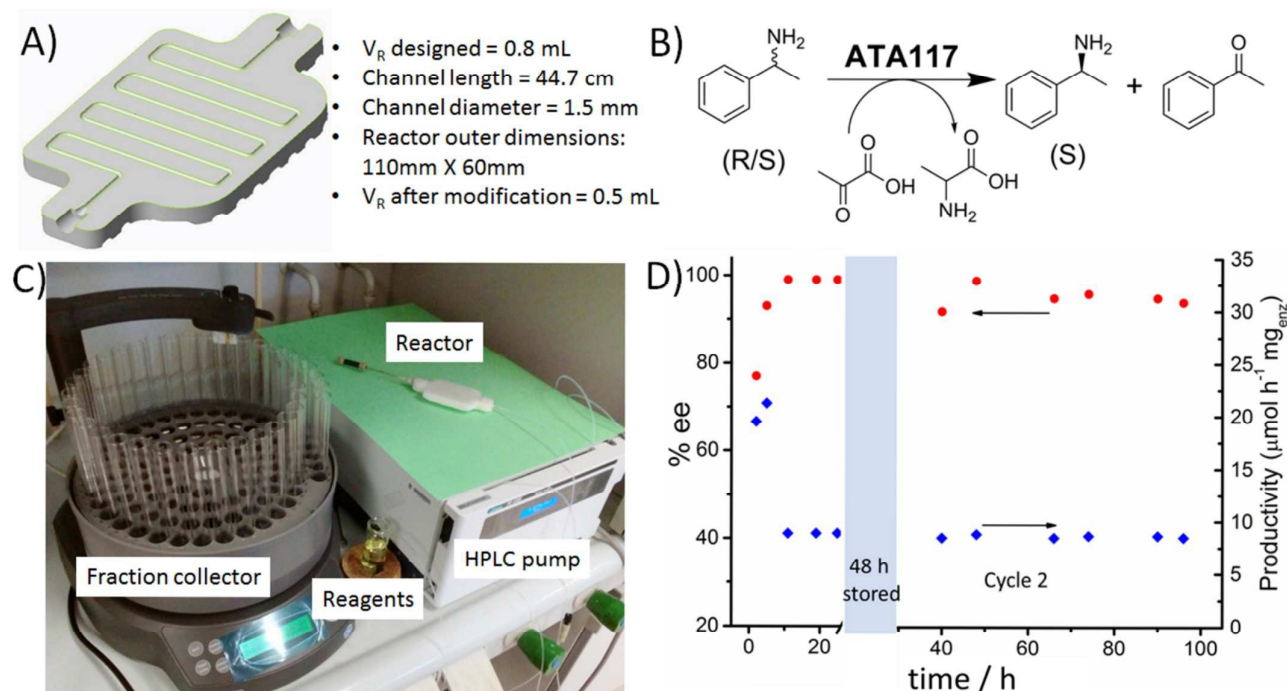


Figure 5. Continuous-flow biocatalytic reactors for the kinetic resolution of *rac*-methylbenzylamine. A) CAD of the bioreactor and main reactor parameters. B) Kinetic resolution of *rac*-methylbenzylamine employing ATA 117 supported on the 3D printed bioreactor. C) Experimental set-up employed for the continuous-flow biocatalytic transformation. D) Productivity and enantiomeric excess observed as a function of time. The first two data points correspond to experiments assayed at $25 \mu\text{L}\cdot\text{min}^{-1}$, while the rest were assayed at $10 \mu\text{L}\cdot\text{min}^{-1}$. The plot represents two separate runs under continuous-flow, the first of them for 24 h, followed by a 48 h storage in fresh buffer and a subsequent run for further 78 h. The results indicate the activity and stability of the enzyme, by keeping its activity over extended periods of time (ca. 100 h) under continuous-flow streams.

The results obtained for the kinetic resolution of *rac*-methylbenzylamine are summarized in Figure 5D. At the initial flow rate assayed $25 \mu\text{L}\cdot\text{min}^{-1}$ of a solution of 5mM *rac*-methylbenzylamine, 5mM pyruvic acid and 0.1mM PLP and after 5 h of time on stream, a conversion of the 48% of the (*R*) enantiomer on the amine into ketone was observed. Thus, (*S*)-methylbenzylamine was obtained with an enantiomeric excess of $93 \pm 2\%$ *e.e.*, as determined by HPLC. This corresponds to a remarkably low residence time of 20 min and a productivity of $20.5 \mu\text{mol h}^{-1} \text{mg}_{\text{enz}}^{-1}$. This is comparable to the batch experiment performed under similar conditions, thus indicating that the enzyme activity is retained. Then, the flow rate was reduced to $10 \mu\text{L}\cdot\text{min}^{-1}$ in order to test the temporal stability of the bioreactor and the reaction was carried out for an additional 20 hours. At this flow rate, corresponding to a residence time of 50 min, almost full conversion of the (*R*)-enantiomer was observed ($>49\%$) yielding the (*S*)-amine with an enantiomeric excess $>99\%$ *e.e.* In order to evaluate the stability of the biocatalytic system, the reactor was flushed with buffer and stored at 4°C for 48 hours. Afterwards, a second cycle was performed under the same experimental conditions ($10 \mu\text{L}\cdot\text{min}^{-1}$, 5mM *rac*-methylbenzylamine, 5mM pyruvic acid, 0.1mM PLP) and the flow system was maintained for a further 78 hours. During these period, the activity and enantioselectivity of the bioreactor was maintained with *e.e.* $>94\%$. These results demonstrate that the enzyme can be effectively immobilized on printed flow bioreactors, and the

productivity of the system is greatly enhanced by the flow conditions. Indeed, a total of 105 catalytic cycles were performed with the same enzyme. This work has demonstrated the first example of enzyme immobilization on modified 3D printed continuous flow biocatalytic reactors and paves the way for numerous applications in industrial biotechnology. The possibility of rapidly testing different immobilization mechanisms and conditions, that are easily transferred to continuous-flow bioreactors with tailored geometries will allow for the development of numerous applications. Significantly, the ω -TA enzymes tested showed a comparable activity to the free enzyme and were successfully recycled. Next steps will include demonstrating the approach on a diverse set of enzymes, employing different printing techniques and assessing alternative immobilisation methods by modifying the surface linking agents.

Acknowledgements

The authors acknowledge the Royal Society (RG150021) for funding and the Research Priority Area (RPA) of UoN in Industrial Biotechnology for funding. Research leading to these results has also received funding from the BBSRC (BB/M021947/1). This work was partially supported by G. V. (PROMETEO 2016-071) and MINECO (CTQ2015-68429R). E. Peris thanks MICINN for personal financial support (FPU13/00685).

References

- 1 A. Schmid, J. S. Dordick, B. Hauer, A. Kiener, M. Wubbolts and B. Witholt, *Nature*, 2001, **409**, 258-268.
- 2 D. J. C. Constable, P. J. Dunn, J. D. Hayler, G. R. Humphrey, J. J. L. Leazer, R. J. Linderman, K. Lorenz, J. Manley, B. A. Pearlman, A. Wells, A. Zaks and T. Y. Zhang, *Green Chem.*, 2007, **9**, 411-420.
- 3 U. T. Bornscheuer, G. W. Huisman, R. J. Kazlauskas, S. Lutz, J. C. Moore and K. Robins, *Nature*, 2012, **485**, 185-194.
- 4 R. A. Sheldon and S. van Pelt, *Chem. Soc. Rev.*, 2013, **42**, 6223-6235.
- 5 a) P. Lozano, *Green Chem.*, 2010, **12**, 555-569; b) P. Lozano, E. Garcia-Verdugo, R. Piamtongkam, N. Karbass, T. De Diego, M. I. Burguete, S. V. Luis, J. L. Iborra, *Adv. Synth. Catal.*, 2007, **349**, 1077-1084.
- 6 R. C. Rodrigues, C. Ortiz, A. Berenguer-Murcia, R. Torres and R. Fernandez-Lafuente, *Chem. Soc. Rev.*, 2013, **42**, 6290-6307.
- 7 I. Gibson, D. W. Rosen and B. Stucker, *Additive Manufacturing Technologies: Rapid Prototyping to Direct Digital Manufacturing*, Springer-Verlag Berlin, Berlin, 2010.
- 8 M. D. Symes, P. J. Kitson, J. Yan, C. J. Richmond, G. J. T. Cooper, R. W. Bowman, T. Vilbrandt and L. Cronin, *Nat. Chem.*, 2012, **4**, 349-354.
- 9 S. Rossi, R. Porta, D. Brenna, A. Puglisi and M. Benaglia, *Angew. Chem. Int. Ed.*, 2017, **56**, 4290-4294.
- 10 O. Okafor, A. Weilhard, J. A. Fernandes, E. Karjalainen, R. Goodridge and V. Sans, *Reaction Chem. Eng.*, 2017, **2**, 129-136.
- 11 V. Dragone, V. Sans, M. H. Rosnes, P. J. Kitson and L. Cronin, *Beilstein J. Org. Chem.*, 2013, **9**, 951-959.
- 12 P. J. Kitson, M. H. Rosnes, V. Sans, V. Dragone and L. Cronin, *Lab Chip*, 2012, **12**, 3267-3271.
- 13 A. K. Au, W. Huynh, L. F. Horowitz and A. Folch, *Angew. Chem. Int. Ed.*, 2016, **55**, 3862-3881.
- 14 Q. Guo, X. Cai, X. Wang and J. Yang, *J. Molec. Chem. B Enzym.*, 2013, **1**, 6644-6649.
- 15 E. Fatarella, D. Spinelli, M. Ruzzante and R. Pogni, *J. Molec. Chem. B Enzym.*, 2014, **102**, 41-47.
- 16 P. Lozano and J. L. Iborra, in *Immobilization of Enzymes and Cells*, ed. G. F. Bickerstaff, Humana Press, Totowa, NJ, 1997, DOI: 10.1385/0-89603-386-4:27, pp. 27-40.
- 17 F. H. Isgrove, R. J. H. Williams, G. W. Niven and A. T. Andrews, *Enzym. Microb. Technol.*, 2001, **28**, 225-232.
- 18 R. D. Goodridge, C. J. Tuck and R. J. M. Hague, *Prog. Mat. Sci.*, 2012, **57**, 229-267.
- 19 A. P. Green, N. J. Turner and E. O'Reilly, *Angew. Chem. Int. Ed.*, 2014, **53**, 10714-10717.
- 20 E. O'Reilly, C. Iglesias and N. J. Turner, *ChemCatChem*, 2014, **6**, 992-995.
- 21 E. O'Reilly, C. Iglesias, D. Ghislieri, J. Hopwood, J. L. Galman, R. C. Lloyd and N. J. Turner, *Angew. Chem. Int. Ed.*, 2014, **53**, 2447-2450.
- 22 L. Martinez-Montero, V. Gotor, V. Gotor-Fernandez and I. Lavandera, *Green Chem.*, 2017, **19**, 474-480.
- 23 M. Lopez-Iglesias, D. Gonzalez-Martinez, V. Gotor, E. Busto, W. Kroutil and V. Gotor-Fernandez, *ACS Catal.*, 2016, **6**, 4003-4009.
- 24 F. Guo and P. Berglund, *Green Chem.*, 2017, **19**, 333-360.
- 25 M. Planchestainer, M. L. Contente, J. Cassidy, F. Molinari, L. Tamborini and F. Paradisi, *Green Chem.*, 2017, **19**, 372-375.
- 26 N. Miložič, M. Lubej, M. Lakner, P. Žnidaršič-Plazl and I. Plazl, *Chem. Eng. J.*, 2017, **313**, 374-381.
- 27 W. Neto, M. Schürmann, L. Panella, A. Vogel and J. M. Woodley, *J. Mat. Chem. B Enzym.* 2015, **117**, 54-61.
- 28 L. H. Andrade, W. Kroutil and T. F. Jamison, *Org. Lett.*, 2014, **16**, 6092-6095.
- 29 P. J. Kitson, R. J. Marshall, D. L. Long, R. S. Forgan and L. Cronin, *Angew. Chem. Int. Ed.*, 2014, **53**, 12723-12728.
- 30 B. Brandt, A. Hidalgo and U. T. Bornscheuer, *Biotech. J.*, 2006, **1**, 582-587.